



Optoelectronically suitable graphene oxide-decorated titanium oxide/polyaniline hybrid nanocomposites and their enhanced photocatalytic activity with methylene blue and rhodamine B dye

Shyamal Baruah¹ · Sudhir Kumar¹ · Bharat Nayak¹ · Amrit Puzari¹

Received: 21 October 2019 / Revised: 2 March 2020 / Accepted: 20 March 2020 /
Published online: 30 March 2020
© Springer-Verlag GmbH Germany, part of Springer Nature 2020

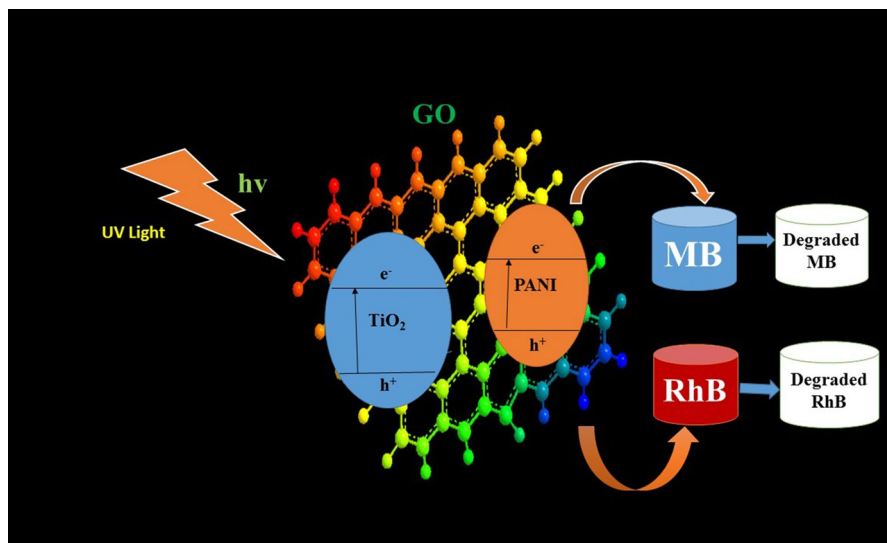
Abstract

Organic–inorganic photocatalytic hybrid nanocomposites based on titanium oxide nanoparticle and polyaniline decorated with graphene oxide were synthesized via in situ chemical oxidative method using ammonium persulphate as an initiator and different weight percentages of TiO₂ nanoparticles. The materials were characterized by using conventional techniques like UV–vis spectroscopy, FT-IR spectroscopy and X-ray diffraction. The electrical conductivity of the nanocomposites was found in the range of semiconducting materials. The nanocomposites possess broad application prospects covering the field of semiconducting devices, solar cells, sensors, microwave-absorbing materials and so on. The nanocomposites also exhibit promising photocatalytic activity towards degradation of methylene blue (MB) and rhodamine B dye in the presence of UV-light radiation. Compared to pure PANI and TiO₂ nanoparticles, the GO/PANI/TiO₂ nanocomposite showed much improvement in degradation efficiency. Significant photodegradation was observed with the molecules where 98.9% degradation was noted with 20% of TiO₂ nanoparticles within 1 h under short-wavelength UV-light.

✉ Amrit Puzari
amrit09us@yahoo.com

¹ Department of Chemistry, National Institute of Technology Nagaland, Chumukedima, Dimapur, Nagaland 797103, India

Graphic abstract



Keywords GO/PANI/TiO₂ nanocomposite · Photocatalysis · Optoelectronics · Fluorescence emitter · Semiconductor · TiO₂ NPs

Introduction

In the past few decades, air and water pollution by organic dyes has become a matter of serious concern due to their high toxicity to aquatic creatures and carcinogenic and mutagenic effects on humans [1]. The large amount of synthetic/organic dyes such as rhodamine, carmine, phenolic, thymol blue, eriochrome black-T (EBT) and methylene blue [2, 3] contained in industrial waste cause serious water pollution during the manufacture in chemical industries that includes paper, textile, leather, food, hair dyes, etc. [4]. Removal of these organic dyes from polluted water bodies is a matter of serious environmental concern, and the development of new advanced photocatalytic materials capable of effectively decomposing those dyes can be an amicable solution [5, 6]. Various metal oxides such as TiO₂ [7], ZnO [8], Cu₂O [9], MnO₂ [10], Fe₂O₃ [11], WO₃ [12] and CeO₂ [13] are used as photocatalysts for the degradation of organic dyes as well as in photoelectrochemical water splitting [14]. Among these, TiO₂ nanoparticles (NPs) have known photocatalytic effectiveness for such applications. Apart from catalytic degradation of dye pollutants, structural, morphological and textural characteristics of TiO₂ also allow this oxide to be used for several other applications such as solar cells [15], batteries [16] and sensors [17]. Other important characteristics of TiO₂ are high chemical stability, strong oxidizing ability, non-toxicity, mechanical robustness and low cost. The efficient photocatalytic activity

under ultraviolet light is often linked with the creation of holes in the valence band through the promotion of electrons to the conduction bands, which in fact is responsible for oxidizing and reducing the dye pollutants [18]. Polymeric materials such as polyaniline, polypyrrole, polythiophene and polyacetylene can effectively adsorb many pollutants [19, 20]. The nanocomposites of polyaniline and polypyrrole modified with TiO_2 nanoparticles are found better than TiO_2 nanoparticle in the degradation of organic dyes [21–23]. Graphene oxide, on the other hand, has attractive optical properties, fluorescence labels, high dispersibility in various polar solvents and the ability to attach diverse molecular structures on its surface (e.g. by hydrogen bonding) [24]. These properties facilitate the adsorption of various molecular structures on its surface, leading to better control of the size, and the shape of the formed structures. These remarkable properties are extremely beneficial in making TiO_2/GO nanocomposites. The relative hydrophilicity of GO, due to the highly oxygenated surface, facilitates its interaction with aqueous dispersions of TiO_2 , leading to the formation of strong chemically bonded TiO_2/GO nanocomposites [25–27].

Polymeric matrixes encapsulated with metallic nanoparticles generally exhibit enhanced thermal stability, electrocatalysis, sensing, microelectronic and excellent photocatalytic properties [28]. Present work demonstrates the synthesis of GO-decorated PANI/ TiO_2 nanocomposites, its structural characterization, investigation of its application prospect towards photocatalytic degradation of methylene blue and rhodamine B dye and evaluation of electrical and fluorescence properties of the materials. The morphological study of such nanocomposites often reveals important structural information that is suitable for making an understanding of their application prospects.

Experimental

Materials

Titanium tetra-isopropoxide, graphene oxide (GO), polyaniline (PANI), ammonium persulfate (APS) and hydrochloric acid were procured from TCI, Japan and Sigma-Aldrich. Graphene oxide and polymer nanocomposites with different weight percentages of titanium dioxide (TiO_2) NPs were characterized by using spectroscopic techniques such as FT-IR spectroscopy, XRD, UV–visible spectroscopy, field emission scanning electron microscope (FESEM) and thermogravimetric analysis (TGA). RIGAKU Ultima IV X-ray diffractometer was used for XRD data processing. For the FT-IR spectra single beam, Fourier transform infrared spectrometer (carry 630 FT-IR) was used at room temperature in the range $400\text{--}4000\text{ cm}^{-1}$. For the study of photoluminescence properties, Cary Eclipse fluorescence spectrometer was used. Similarly, for the UV–visible absorption spectra, Carry 100 UV–visible spectrophotometer was used within the wavelength range of $200\text{--}800\text{ nm}$. Dye degradation was studied under short-wavelength ultraviolet light (250 nm).

Synthesis of TiO₂ nanoparticle (sol–gel process)

TiO₂ nanoparticles were synthesized via the sol–gel method, where titanium tetra-isopropoxide, Ti[(OCH(CH₃)₂)]₄ and iso-propanol (CH₃)₂CHOH were used as precursors without any further purification using reported literature procedure [29].

Synthesis of polyaniline

Aniline (3.0 mmol) was dissolved in a 50 ml aqueous solution of 1 M HCl and ultrasonicated for 30 min to get the homogeneous solution at 50 °C. Ammonium persulphate (APS) (6.0 mmol) was dissolved in 10 ml of 1 M HCl and further added slowly to the above solution and ultrasonicated it for 2.5 h. After the formation of the product, the reaction mixture was filtered and washed with 1 M HCl and deionized water and was dried finally at 60 °C in hot air oven [30].

Synthesis of GO/PANI/TiO₂ nanocomposites

Synthesis of GO-decorated TiO₂ and PANI-wrapped nanocomposite was performed by in situ oxidative polymerization of aniline keeping the feed amount of aniline and GO. Aniline 0.3 ml was dissolved in a 50 ml aqueous solution of 1 M HCl and ultrasonicated for 20 min. 100 mg of GO was dispersed in this solution and ultrasonicated for 20 min. Then, a calculated amount of TiO₂ nanoparticle (25, 50, 75 and 100 mg) was dispersed in this solution and ultrasonicated for 20 min at 50 °C. The oxidant solution was prepared by dissolving 1.5 gm APS in 10 ml of 1 M HCl. The solution was added dropwise to the reaction mixture under ultrasonication. The reaction mixture was ultrasonicated for 2.5 h in a water bath at 50 °C. Finally, the product was filtered and washed with 1 M HCl (1 × 5 ml) and deionized water (3 × 5 ml) and dried in a hot air oven at 60 °C overnight [31].

Results and discussion

In hybrid materials like GO/PANI/TiO₂ nanocomposites, various inorganic particles are combined with the conducting polymers via some chemical and/or electrochemical techniques. Such types of nanoparticles, possessing different sizes and nature, are used to obtain materials with varying physical properties. GO-based polymer nanocomposites were successfully synthesized using different percentages of titanium dioxide nanoparticles. Spectroscopic characterization of the materials strongly supports the formation of these polymeric nanocomposites. Synthesis of the polymer nanocomposites was accomplished by using the reported polymerization technique for oxidative in situ polymerization of polyaniline.

FT-IR Spectrum of TiO₂ nanoparticle

FT-IR spectra of TiO₂ nanoparticle exhibit strong metal oxide peak at 422 cm⁻¹ for O–Ti–O bonding in anatase morphology, as shown in Fig. 1. This observation confirms the formation of TiO₂ nanoparticles. The bands centred at 1650 cm⁻¹ and 3380 cm⁻¹ are the characteristics of surface-adsorbed water and hydroxyl groups, which are the characteristic of δ-H₂O bending and vibration of hydroxyl groups [32].

XRD pattern of TiO₂ nanoparticle

In case of TiO₂ nanoparticles (Fig. 2), the diffraction peaks were observed at 2θ values of 25.56°, 37.11°, 38.21°, 48.19°, 54.17°, 55.29°, 62.61°, 69.03°, 70.35° and 75.02° and were identified to originate from (101), (103), (004), (200), (105), (211), (204), (116), (220) and (215) planes which are matching with the standard JCPDS data. The crystallite size of the nanoparticles was calculated as 15.91 nm using the Scherer equation and thus confirms the formation of TiO₂ nanoparticles. The strong peak is observed at 2θ value of 25.56° confirms the TiO₂ anatase structure [33].

FT-IR spectroscopy of GO/PANI and GO/PANI/TiO₂ nanocomposites

FT-IR spectra recorded for GO/PANI and GO/PANI/TiO₂ nanocomposites with 5, 10, 15 and 20 weight percentages of TiO₂ NPs are depicted in Fig. 3(1–2). In the GO/PANI IR spectra, the peak observed at 3205 cm⁻¹ is due to N–H stretching vibrations of the -NH-group of PANI. But for the nanocomposites, this peak shifted to 3225 cm⁻¹. Another peak at 2659 cm⁻¹ in GO/PANI may be due to the symmetrical and asymmetrical N–H stretching of -NH₂ group. While for the

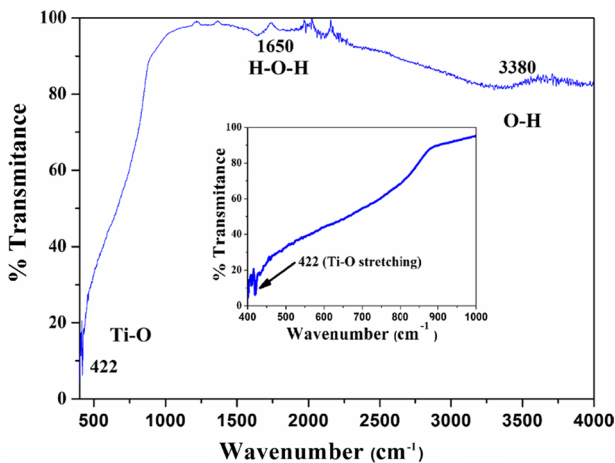


Fig. 1 FT-IR spectrum of TiO₂ nanoparticles

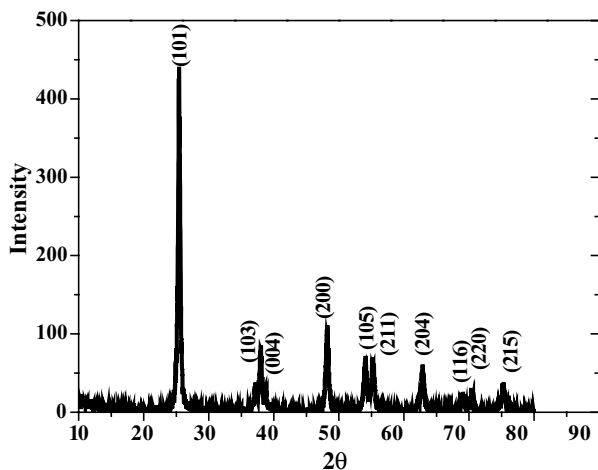


Fig. 2 XRD pattern of TiO_2 nanoparticles

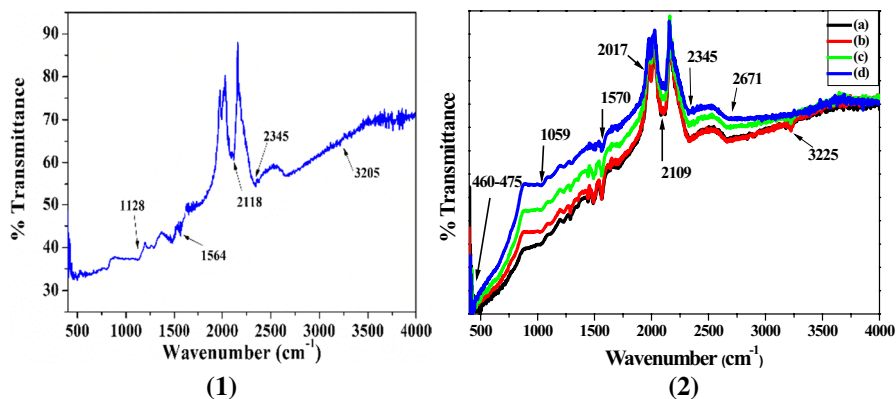


Fig. 3 FT-IR spectra of (1) GO/PANI and (2) GO/PANI/ TiO_2 nanocomposites with **a** 5%, **b** 10%, **c** 15% and **d** 20% of TiO_2 NPs by weight

nanocomposites, a clear shifting of the peak was observed to 2671 cm^{-1} . Similarly for GO/PANI, the peak observed at 1564 cm^{-1} and 1500 cm^{-1} can be attributed to C=N and C=C stretching vibration of phenazine ring. But for the nanocomposites, the C=N peak also shifted to 1570 cm^{-1} . The reason behind these shifting is due to the incorporation of TiO_2 into the polymer matrix. Similarly, other peaks at $1000\text{--}1200\text{ cm}^{-1}$ can be assigned to the C–N stretching mode of the benzenoid ring. In addition to the above peaks, the peak at $400\text{--}450\text{ cm}^{-1}$ confirms the incorporation of TiO_2 into the GO/PANI matrix [34].

XRD analysis of GO/PANI/TiO₂ nanocomposites

The XRD spectra of GO/PANI/TiO₂ nanocomposites for four different weight percentages of TiO₂ (5%, 10%, 15% and 20%) are shown in Fig. 4. The small peak at $2\theta=10.7^\circ$ corresponds to (0 0 1) crystal plane of graphene oxide. XRD peaks at $2\theta=25.32^\circ$, 37.66° , 48.13° , 53.92° , 55.30° , 63.66° , 69.03° , 70.32° and 75.03° are assigned, respectively, to the diffractions of the (1 0 1), (0 0 4), (2 0 0), (1 0 5), (2 1 1), (2 0 4), (1 1 6), (2 2 6) and (2 1 5) crystal planes of anatase phase based on TiO₂ nanoparticle. The appearance of the peaks at an identical position for the four different compositions indicates that the state of TiO₂ did not change during the polymerization process [35]. The XRD peak of PANI at 20.72° and 25.23° in the composites becomes less obvious as it is overlapped with the sharp crystalline peak of TiO₂ [36]. The average semicrystalline size of the polymer nanocomposites calculated by the Scherer equation is $t=20.36$ nm to 28 nm. XRD pattern comparison shows that there is no significant change in the crystalline structure of TiO₂ due to its dispersion in GO and PANI during polymerization.

UV–visible spectroscopy of GO/PANI/TiO₂ nanocomposites

The UV–visible spectra of GO/PANI/TiO₂ nanocomposites are shown in Fig. 5. From the figure, two major absorption peaks can be observed at 265 nm and 375 nm. The first peak at 265 nm is due to $\pi-\pi^*$ electron transitions within the benzenoid and quinoid segments of the polyaniline [37]. The band observed at 375 nm originates from the generation of charged species polaron (polaron $-\pi^*$ transition).

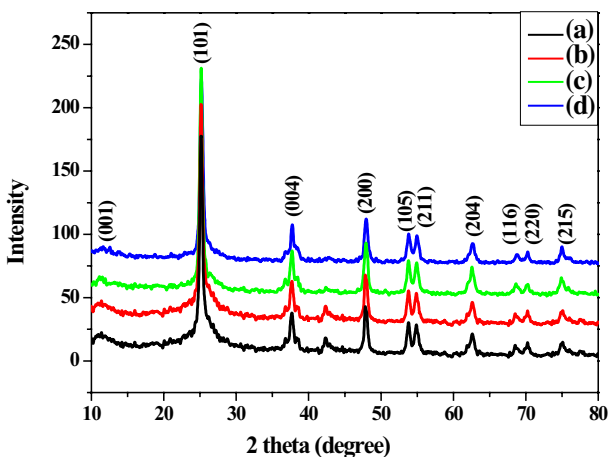


Fig. 4 XRD analysis of GO/PANI/TiO₂ nanocomposites with **a** 5%, **b** 10%, **c** 15% and **d** 20% of TiO₂ NPs by weight

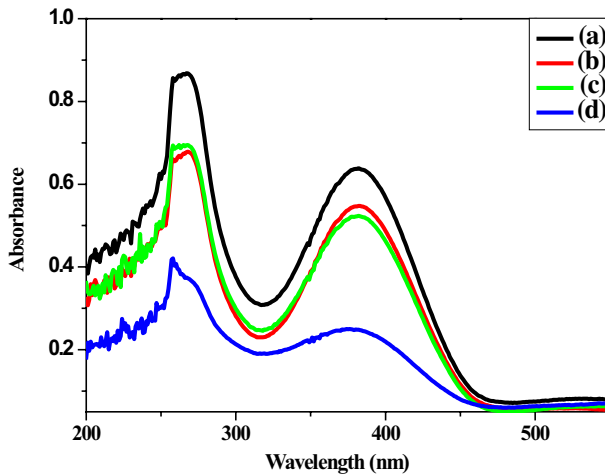
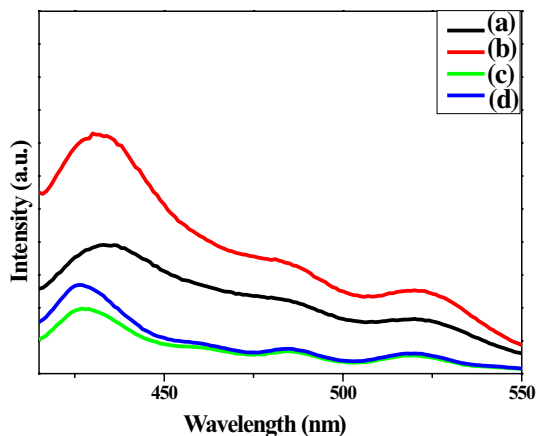


Fig. 5 UV–visible spectra of GO/PANI/TiO₂ nanocomposites with a 5%, b 10%, c 15% and d 20% of TiO₂ NPs by weight

Photoluminescence spectra of GO/PANI/TiO₂ nanocomposites

Illumination with UV or visible light leads to the generation of photons from the recombination of photoinduced electrons and positively charged holes. Because of this fact, a substance produces the characteristic PL peak. The photoluminescence spectra of GO/PANI/TiO₂ nanocomposites with different ratios of TiO₂ can be depicted in Fig. 6. The broad peak 400–425 nm shown in Fig. 6 falls in the range of violet emitter. Here we can say that the violet light emitter range of nanocomposites increases after the addition of TiO₂ nanoparticle [38]. We have also observed that the presence of graphene oxide broadens the photosensitization

Fig. 6 Photoluminescence spectra of GO/PANI/TiO₂ nanocomposites with a 5%, b 10%, c 15% and d 20% of TiO₂ NPs by weight



band of TiO_2 and forms the Ti-O-C chemical bond which will accelerate the photocatalytic efficiency of the composite.

Thermogravimetric analysis (TGA) of GO/PANI/ TiO_2 nanocomposites

Thermograms obtained for GO/PANI/5% TiO_2 , GO/PANI/10% TiO_2 , GO/PANI/15% TiO_2 and GO/PANI/20% TiO_2 nanocomposites are shown in Fig. 7. The figure indicates three stages of thermal decompositions for all the nanocomposites. The initial dehydrating stage at 45–100 °C may be due to the desorption of water and ethanol absorbed in the polymer surface. The second weightloss stage from 180 to 250 °C is due to the degradation of the oligomers or side products present in the composite materials. The third and final transition is observed from 260 °C onwards due to the degradation of benzenoid and quinonoid repeating units of the polymeric backbone of graphene oxide and polyaniline [39]. The thermal stability of GO/PANI/ TiO_2 nanocomposites increases progressively with an increase in the weight percentage of TiO_2 nanoparticles in the composite materials.

FESEM analysis of GO/PANI/ TiO_2 nanocomposites

Surface morphology and adhesion behaviour of the nanocomposites were investigated through FESEM characterization. Field emission scanning electron microscopy images of GO/PANI/ TiO_2 nanocomposites with 5, 10, 15 and 20 weight percentages of TiO_2 NPs are represented in Fig. 8a–d. As we have seen from the figure, the TiO_2 nanoparticles are homogeneous and crack-free along the whole surface and show good adhesion to the substrate. We can also distinctly observe that GO/PANI

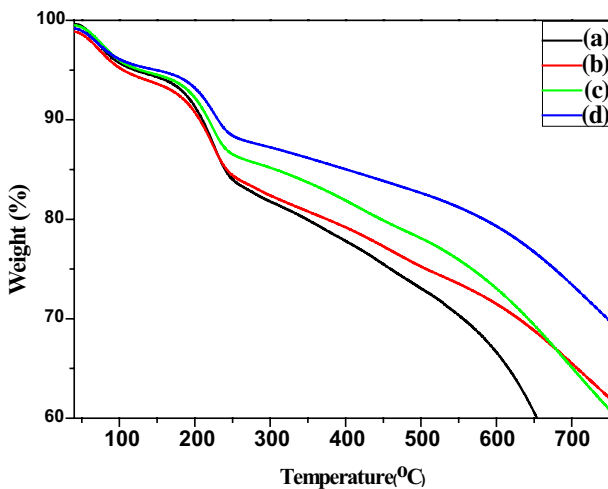


Fig. 7 TGA spectra of GO/PANI/ TiO_2 nanocomposites with **a** 5%, **b** 10%, **c** 15% and **d** 20% of TiO_2 NPs by weight

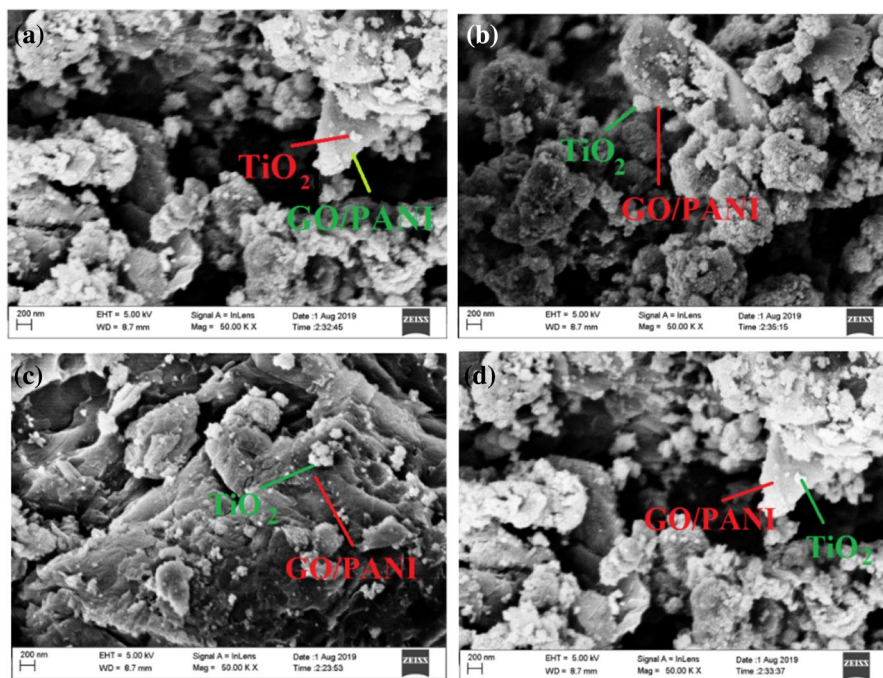


Fig. 8 a–d FESEM image of GO/PANI/TiO₂ nanocomposites with **a** 5, **b** 10, **c** 15 and **d** 20 weight percentage of TiO₂ NPs

surface is coated with a smooth thin TiO₂ layer and some regions of the surface of GO sheets deposited with polyaniline [40].

Electrical conductivity of GO/PANI/TiO₂ nanocomposites

I–V characteristics for an electrical component generally describe a relation between the current and the voltage across it. From the I–V characteristic, along with current respective to voltage, we can also determine breakdown voltage, current of electronics devices, suitable protection, losses and heating of devices (Fig. 9).

Keeping the above facts in mind, the electrical characterization (I–V measurement) of GO/PANI/metal oxide nanocomposites was carried out. From the I–V data, the conductivities were evaluated using bulk resistance (R_b) and using the formula

$$\sigma = (t/A)(1/R_b) \text{ S/cm}$$

where t is the thickness of the pellet, A is the area of pellet and R_b is the bulk resistance of the pellet.

The conductivity data calculated for GO/PANI/TiO₂ composites with a different weight percentage of TiO₂ nanoparticles from the I–V measurements are shown in Table 1.

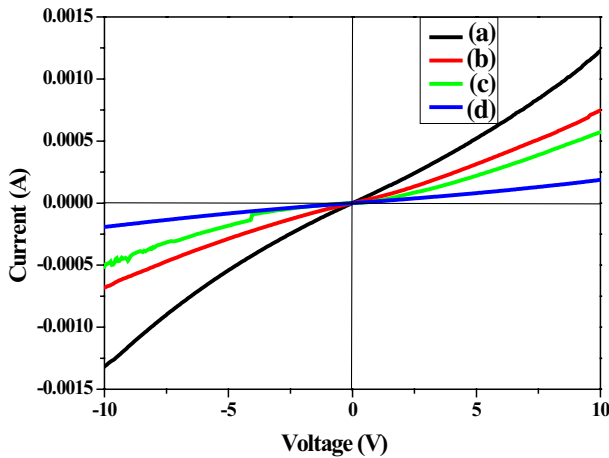


Fig. 9 I–V characteristics of GO/PANI/TiO₂ nanocomposites with **a** 5%, **b** 10%, **c** 15% and **d** 20% of TiO₂ NPs by weight

Table 1 Conductivity and resistivity of of GO/PANI/TiO₂ nanocomposites with **a** 5%, **b** 10%, **c** 15% and **d** 20% of TiO₂ NPs by weight

Compound	<i>t</i> (cm)	<i>A</i> (cm ²)	<i>R</i> _b (ohm)	Resistivity (ohm-cm)	Conductivity (S/cm)
GO/PANI/5% TiO ₂ NCs	.1	1.32	6.94 × 10 ⁻⁶	1.09 × 10 ⁴	9.1 × 10 ⁻⁵
GO/PANI/10% TiO ₂ NCs	.1	1.32	4.23 × 10 ⁻⁶	1.78 × 10 ⁴	5.6 × 10 ⁻⁵
GO/PANI/15% TiO ₂ NCs	.1	1.32	2.11 × 10 ⁻⁶	3.57 × 10 ⁴	2.8 × 10 ⁻⁵
GO/PANI/20% TiO ₂ NCs	.1	1.32	7.60 × 10 ⁻⁷	9.80 × 10 ⁴	1.02 × 10 ⁻⁵

From Table 1, the electrical conductivity calculated for the GO/PANI/TiO₂ nanocomposites was found of the order of 10⁻⁵ S/cm. With an increase in the ratio of metal oxide nanoparticles, the value of conductivity of the nanocomposites decreases progressively. The reason behind the decrease in conductivity value is that for the nanocomposites, with the increasing amount of TiO₂ there was a decrease in the ratio of PANI/TiO₂. It is well established that PANI is more conductive than TiO₂. Therefore, incorporation of metal oxide nanoparticles results in a decrease in the PANI/TiO₂ ratio which influences the conducting behaviour of the polymeric materials.

Evaluation of photocatalytic activity (methylene blue dye degradation)

Photocatalytic activity of the hybrids with different compositions is evaluated in terms of photodegradation of methylene blue (MB) in aqueous solution under irradiation with UV-light. Semiconductor materials usually possess good photocatalytic efficiency and hence can be used for photodegradation of organic pollutants. Based on this fact, we investigated the photocatalytic efficiency of the

hybrid nanocomposites. For that purpose, we have investigated the photodegradation of methylene blue (MB) dye using the four hybrid nanocomposites separately. We have observed that GO/PANI/TiO₂ hybrid nanocomposites have much higher photocatalytic efficiency compared to TiO₂ nanoparticles and polyaniline alone. This enhanced photocatalytic efficiency of GO/PANI/TiO₂ composite can be attributed to the suppression of electron recombination and the enhancement of mass transportation. Polyaniline upon hybridization with graphene oxide possesses increased dye absorptivity on the surface due to the π - π conjugation between methylene blue and aromatic region of graphene oxide. That also reduces the bandgap leading to extended absorption and significant electron transfer from polyaniline to GO sheets before recombination [41].

Initially, we have studied the photocatalytic efficiency of TiO₂ nanoparticles using 50 ppm concentration MB solution, and the result of the experiment is presented in Fig. 10a. We have observed that TiO₂ nanoparticle provides more than 90% photocatalytic degradation efficiency after 3 h. The degradation occurred due to the electronic transition of TiO₂ nanoparticles by the high-energy ray of light. Similarly, the experiment was also carried out with PANI alone. Figure 10b represents the results of this experiment. It is clearly observed from the figure that the PANI gives up to 40% photocatalytic degradation efficiency in around three hours. On the contrary, experiments carried out with hybrid nanocomposites using the same concentration of methylene blue solution indicate that photocatalytic efficiency of GO/PANI/TiO₂ nanocomposites is much improved compared to the same for TiO₂ nanoparticles or PANI. Results of degradation experiment carried out with methylene blue using the four hybrid nanocomposites are represented in Fig. 10c–f. It has been observed that the GO/PANI/10% TiO₂ nanocomposite possesses up to 95% photocatalytic degradation efficiency in around 2 h. In the same way, the GO/PANI/15%TiO₂ nanocomposite gives up to 98% photocatalytic degradation efficiency in around 80 min only. Even for a higher weight percentage of TiO₂ nanoparticle, for example for the case of GO/PANI/20%TiO₂ nanocomposite, we obtained around 98% photocatalytic degradation efficiency just in forty minutes. In other words, the hybrid nanocomposites possess superior photocatalytic efficiency as compared to TiO₂ or PANI. The measurements were taken after each 10–20-min interval of time, under the short-wavelength UV–visible light and wt% were taken as used for the synthesis procedure.

The degradation behaviour of methylene blue (MB) dye concerning the four hybrid nanocomposites is shown in Fig. 11. It is clearly observed from the figure that the degradation of MB solution obtained was maximum for TiO₂/PANI hybrid composite with 20 wt% load. PANI acts as an effective photosensitizer in the photocatalytic reaction, that can significantly improve the separation efficiency of photo-excited electron–hole pairs. As PANI is an efficient electron donor, it can even be stimulated by UV-light. The generated electrons from PANI can be easily transferred to the conduction band of TiO₂ when photocatalyst is illuminated with UV-light. If the electrons are trapped at the interface of PANI and TiO₂, the efficient charge separation of photo-created electron and hole pairs might occur. In this process, the reactive electrons can reduce O₂ adsorbed on the surface of nanocomposite to O²⁻, which can further transform into H₂O₂ and OH⁻, resulting in finally the oxidation of

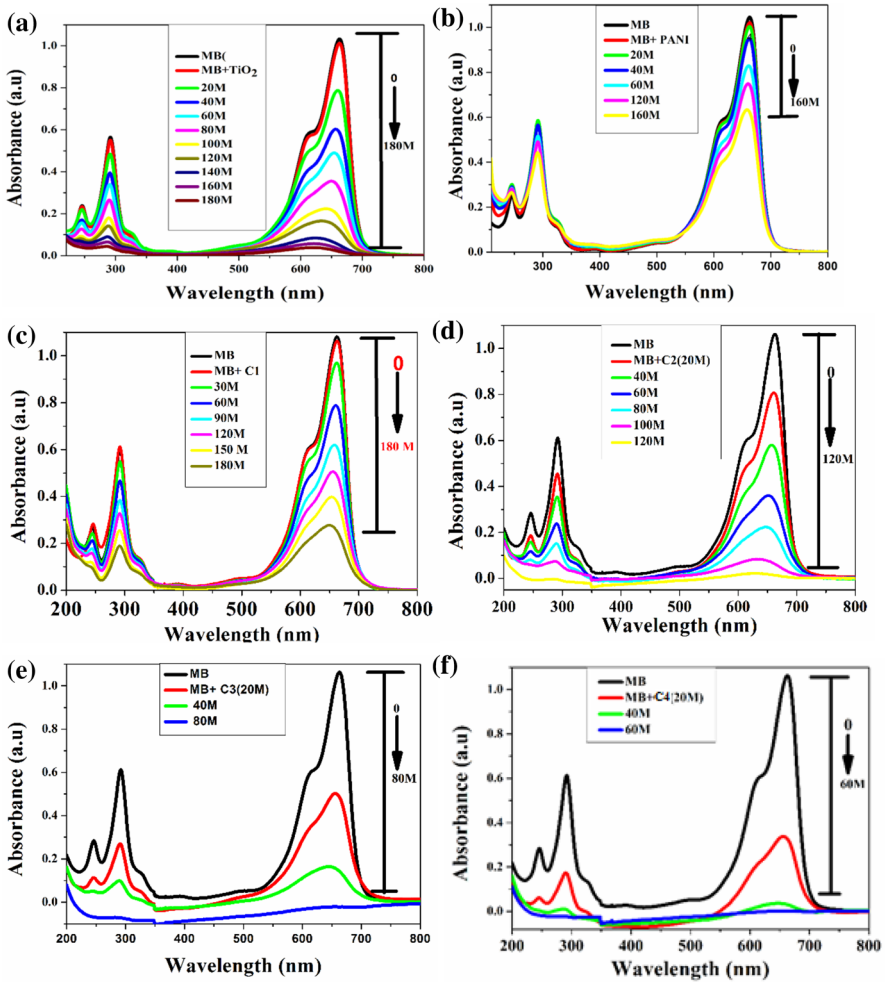


Fig. 10 a–f Photocatalytic degradation of methylene blue dye by using **a** TiO₂, **b** PANI and **c–f** GO/PANI/TiO₂ nanocomposites with 5(C1), 10(C2), 15(C3) and 20(C4) weight percentage of TiO₂ NPs

MB to generate degraded products. As a result, PANI-modified TiO₂ has enhanced photocatalytic activity [42].

Evaluation of photocatalytic efficiency for degradation of rhodamine B dye

Motivated by the results with methylene blue dye, we also investigated the photocatalytic efficiency of rhodamine B dye (RhB), which is often used as a model dye molecule for the study of photocatalytic degradation by transition metal oxide. It shows a major absorption band centred at 553 nm, which is used to monitor the photocatalytic degradation of RhB. The photocatalytic efficiencies of the TiO₂, PANI and GO/

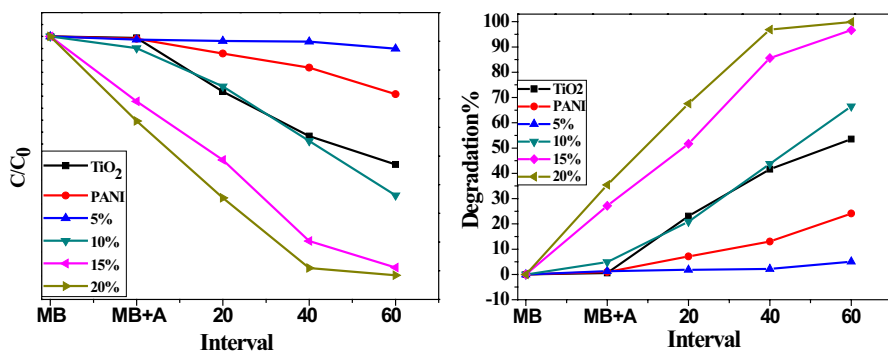


Fig. 11 Degradation behaviour of methylene blue (MB) dye for TiO₂, PANI and nanocomposites (5–20%)

PANI/TiO₂ nanocomposites with different wt% of TiO₂ were evaluated towards the degradation of RhB under UV-light irradiation.

Results presented in Fig. 12a–f once again reveal the fact that graphene oxide-decorated hybrid nanocomposites have much better photocatalytic efficiency as compared to other components of the nanocomposites, i.e. TiO₂ and PANI. From Fig. 12a, which shows the photocatalytic activity of TiO₂ nanoparticle, we can conclude that up to 240 min TiO₂ showed around 75% degradation of the rhodamine B dye. Similarly, from Fig. 12b we observe that PANI showed around 55% degradation in 200 min indicating the superiority of TiO₂ molecule over PANI with respect to photocatalytic efficiency. Figure 12c–f shows the photocatalytic activity of GO/PANI/TiO₂ nanocomposites (5–20%). From the figure, it is clear that 20% nanocomposite is showing the highest activity out of the four composites (5%, 10%, 15% and 20%). The origin of the intense characteristic colour of the RhB dye is due to their conjugated structures constituted with carbonyl, azo and aromatic groups. After the degradation, these groups undergo a successful breakage of their conjugation system in the presence of the GO-PANI/TiO₂ nanocomposite. GO-PANI nanocomposite generally exhibits photo-excited electrons that are transferred from the LUMO level of PANI to the conductive band of the GO. In this way, the GO acts as an acceptor of the photo-excited electrons from PANI which results in the rapid transfer of electrons to the two-dimensional planar structure of GO. Thus, the photogenerated electrons and holes recombination accelerated the suppression and leaves more charge carriers to form on the reactive species, which promotes the degradation of dyes.

Plausible photodegradation mechanism of methylene blue (MB) and rhodamine B (RhB)

The energy levels for lowest unoccupied molecular orbital (LUMO) and highest occupied molecular orbital (HOMO) of PANI are higher compared to the conduction band and valence band position of TiO₂. Upon excitation with visible light, PANI transfers the excited electrons from π -orbital to π^* -orbital, resulting in the creation of a hole in GO/PANI fraction. The excited electrons are then moved from

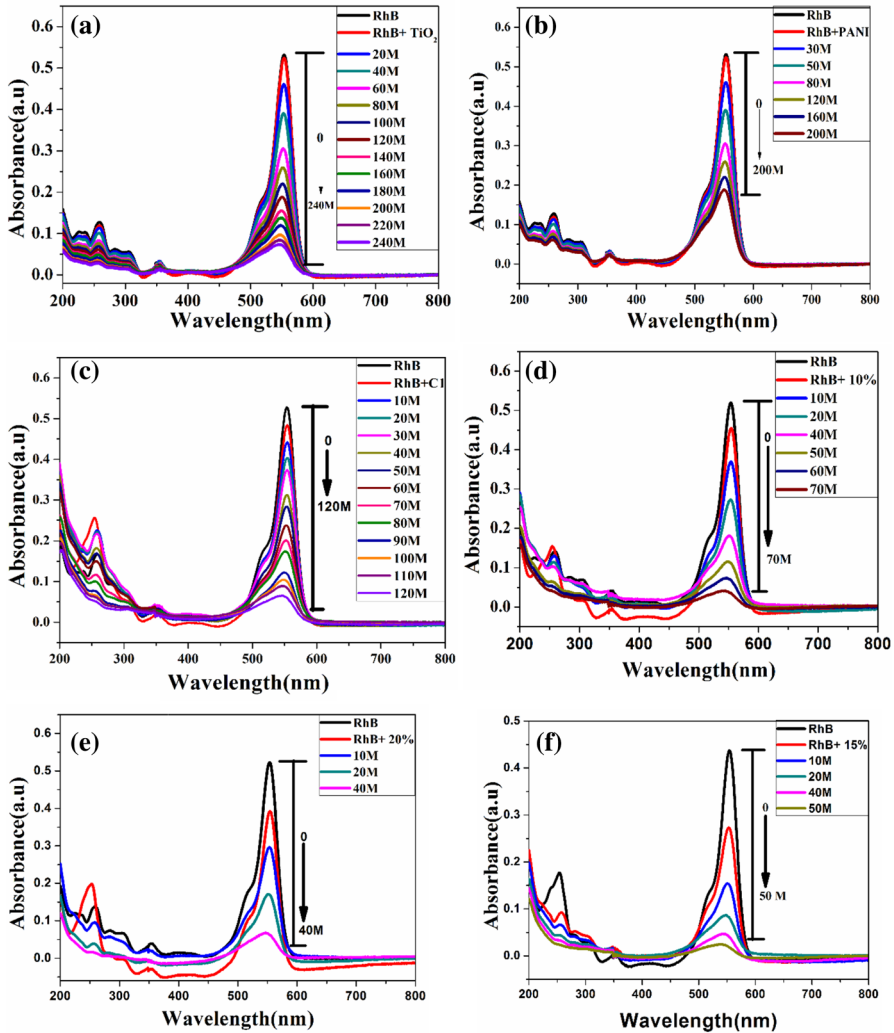
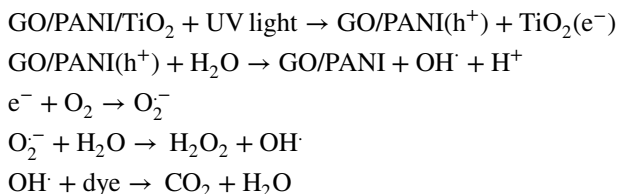


Fig. 12 a–f Photocatalytic degradation of rhodamine B dye by using **a** TiO₂, **b** PANI and **c–f** GO/PANI/TiO₂ nanocomposites with 5(C1), 10(C2), 15(C3) and 20(C4) weight percentage of TiO₂ NPs

LUMO of PANI to the CB of TiO₂. After that, the positively charged GO/PANI fraction reacts with water to produce hydroxyl radicals while the electron reacts with oxygen to produce superoxide radicals. The superoxide radical can further react with water molecules to produce hydrogen peroxide and hydroxyl radical. These radical species finally react with the dye component to produce degraded products, and in this way, the organic pollutants are converted into less toxic materials. Incorporation of graphene oxide (GO) further enhances the photocatalytic property of the nanocomposite. The photogenerated electrons from PANI are separated effectively, which increases the photocatalytic efficiency of nanocomposites [43].



Conclusion

In this study, we have successfully described the formation of stable hybrid nanocomposites of PANI with different weight percentages of TiO₂, decorated with graphene oxide. Incorporation of graphene oxide into the hybrid nanocomposites dramatically improves the photocatalytic efficiency of the nanocomposites towards the degradation of organic dyes such as methylene blue and rhodamine B, under short-wavelength ultraviolet light. Best results have been obtained with the nanocomposite having the highest weight percentage of TiO₂ nanoparticle, i.e. with a 20% weight ratio of TiO₂ nanoparticles. It apparently establishes the fact that these hybrid nanocomposites can be employed for degrading toxic organic pollutants to non-toxic products and therefore can be advocated as a suitable agent for environmental protection. Further, since the observed conductivity of the nanocomposites is well within the range of semiconducting materials, therefore, the nanocomposites are also promising materials for application in the field of electronics and optoelectronics.

References

1. Kim SP, Choi HC (2014) Photocatalytic degradation of methylene blue in presence of graphene oxide/TiO₂ Nanocomposites. *Bull Korean Chem Soc* 35:2660
2. Moghaddam HM, Nasirian S (2014) Hydrogen gas sensing feature of polyaniline/titania (rutile) nanocomposite at environmental conditions. *Appl Surf Sci* 317:117
3. Huang H, Gan M, Li M, Yu L, Hu H, Yang F, Li Y, Ge C (2015) Fabrication of polyaniline/graphene oxide/ titania nanotube arrays nanocomposites and their application in supercapacitors. *J Alloys Compounds* 630:214
4. Hiragond CB, Kshirsagar AS, Khanna DP, More PV, Khanna PK (2018) Electro-photocatalytic degradation of methylene blue dye using various nanoparticles: a demonstration for undergraduates. *J Nanomed Res* 7:254
5. Kampouri S, Nguyen TN, Spodaryk M, Palgrave RG, Züttel A, Smit B, Stylianou KC (2018) Dual-functional photocatalysis: concurrent photocatalytic hydrogen generation and dye degradation using MIL-125-NH₂ under visible light irradiation. *Adv Funct Mater* 28:1
6. Patil MR, Shrivastava VS (2014) Photocatalytic degradation of carcinogenic methylene blue dye by using polyaniline-nickel ferrite nano-composite. *Der Chemica Sinica* 5:8
7. Zapol P, Curtiss LA (2007) Organic molecule adsorption on TiO₂ nanoparticles: a review of computational studies of surface interactions. *J Comput Theo Nanosci* 4:222
8. Saravanan R, Shankar H, Rajasudha G, Stephen A, Narayanan V (2011) Photocatalytic degradation of organic dye using nano ZnO. *Int J Nanosci* 10:253
9. Khattar HK, Jouda AM, Alsaady F (2018) Preparation of Cu₂O nanoparticles as a catalyst in photocatalyst activity using a simple electrodeposition route. *Nano Biomed Eng* 10:406

10. Saravanakumar K, Muthuraj V, Vadive S (2016) Constructing novel Ag nanoparticles anchored on MnO₂ nanowires as an efficient visible light driven photocatalyst. *RSC Adv* 6:61357
11. Liu X, Chen K, Shim JJ, Huang J (2015) Facile synthesis of porous Fe₂O₃ nanorods and their photocatalytic properties. *J Saudi Chem Soc* 19:479
12. Dong P, Hou G, Xi X, Shao R, Dong F (2017) WO₃-based photocatalysts: morphology control, activity enhancement and multifunctional applications. *Environ Sci Nano* 4:539
13. Pourtehdal HR, Kadkhodaie A (2010) Synthetic CeO₂ nanoparticle catalysis of methylene blue photodegradation: kinetics and mechanism. *Chinese J Catal* 31:1328
14. Bagal IV, Chodankar NR, Hassan MA, Waseem A, Johar MA, Kim DH, Ryu SW (2019) Cu₂O as an emerging photocathode for solar water splitting—a status review. *Int J Hydrogen Energ* 44:21351
15. Roose B, Pathak S, Steiner U (2015) Doping of TiO₂ for sensitized solar cells. *Chem Soc Rev* 44:8326
16. Wen W, Wu JM, Jiang YZ, Bai JQ, Lai LL (2016) Titanium dioxide nanotrees for high-capacity lithium-ion microbatteries. *J Mater Chem A* 4:10593
17. Bai J, Zhou B (2014) Titanium dioxide nanomaterials for sensor applications. *Chem Rev* 114:10131
18. Stucchi M, Bianchi CL, Pirola C, Vitali S, Cerrato G, Morandi S, Argiris C, Sourkouni G, Sakkas PM, Capucci V (2015) Surface decoration of commercial micro-sized TiO₂ by means of high energy ultrasound: a way to enhance its photocatalytic activity under visible light. *Appl Catal B Environ* 178:124
19. Li C, Wang J, Guo H (2015) Low temperature synthesis of polyaniline crystalline TiO₂-halloysite composite nanotubes with enhanced visible light photocatalytic activity. *J Colloid Interface Sci* 458:1
20. Heeger AJ (2010) Semiconducting polymers: the third generation. *Chem Soc Rev* 39:2354
21. Lin Y, Li D, Hu J, Xiao G, Wang J, Li W, Fu X (2012) Highly efficient photocatalytic degradation of organic pollutants by PANI-modified TiO₂ composite. *J Phys Chem C* 116:5764
22. Dimitrijevic NM, Tepavecic S, Liu Y, Rajh T, Silver SC, Tiede DM (2013) Nanostructured TiO₂/polypyrrole for visible light photocatalysis. *J Phys Chem C* 117:15540
23. Muktha B, Madras G, Guru Row TN, Scherf U, Patil S (2007) Conjugated polymers for photocatalysis. *J Phys Chem B* 111:7994
24. Tayel A, Ramadan AR, Seoud OAE (2018) Titanium dioxide/graphene and titanium dioxide/graphene oxide nanocomposites: synthesis, characterization and photocatalytic applications for water decontamination. *Catalysts* 8:491
25. Chen D, Feng H, Li J (2012) Graphene oxide: preparation, functionalization, and electrochemical applications. *Chem Rev* 112:6027
26. Zhu Y, Murali S, Cai W, Li X, Suk JW, Potts JR, Ruoff RS (2010) Graphene and graphene oxide: synthesis, properties, and applications. *Adv Mater* 22:3906
27. Dreyer DR, Park S, Bielawski CW, Ruoff RS (2010) The chemistry of graphene oxide. *Chem Soc Rev* 39:228
28. Reddy KR, Karthik KV, Prasad SSB, Soni SK, Jeong HM, Raghu AV (2016) Enhanced photocatalytic activity of nanostructured titanium dioxide/polyaniline hybrid photocatalysts. *Polyhedron* 120:169
29. Sharma A, Karn RK, Pandiyan SK (2014) Synthesis of TiO₂ nanoparticles by sol–gel method and their characterization. *J Basic Appl Eng Res* 1:1
30. Boeva ZA, Sergeev VG (2014) Polyaniline: synthesis, properties, and application. *Pol Sci Ser C* 56:144
31. Vadivel S, Theerthagiri J, Madhavan J, Maruthamani D (2016) Synthesis of Polyaniline/graphene oxide composite via ultrasonication method for photocatalytic applications. *Mater Focus* 5:393
32. Yu JC, Zhang LZ, Zheng Z, Zhao JC (2003) Synthesis and characterization of phosphated mesoporous titanium dioxide with high photocatalytic activity. *Chem Mater* 15:2280
33. Ba-Abbad M, Kadhum AH, Mohamad A, Takriff MS, Sopian K (2012) Synthesis and catalytic activity of TiO₂ nanoparticles for photochemical oxidation of concentrated chlorophenols under direct solar radiation. *Int J Electrochem Sci* 7:4871
34. Lai C, Li GR, Dou YY, Gao XP (2010) Mesoporous polyaniline or polypyrrole/anatase TiO₂ nanocomposites as anode materials for lithium-ion batteries. *Electrochim Acta* 55:4567
35. Al-Hussaini S, Eltabie RK, Rashad MEE (2016) One-pot modern fabrication and characterization of TiO₂ @terpoly(aniline, anthranilic acid and o-phenylenediamine) core-shell nanocomposites via polycondensation. *Polymer* 101:328

36. Jumat NA, Wai PS, Ching JJ, Basirun WJ (2017) Synthesis of polyaniline-TiO₂ nanocomposites and their application in photocatalytic degradation. *Polym Polym Compos* 25:507
37. Mostafaei A, Zolriasatein A (2012) Synthesis and characterization of conducting polyaniline nanocomposites containing ZnO nanorods. *Progress in Natural Science: Mater. Inter.* 22:273
38. Tao P, Li Y, Rungta A, Schadler LS (2011) TiO₂ nanocomposites with high refractive index and transparency. *J Mater Chem* 21:18623
39. Manivel P, Dhakshnamoorthy M, Balamurugan A, Ponpandian N, Mangalaraj D, Viswanathan C (2013) Conducting polyaniline-graphene oxide fibrous nanocomposites: preparation, characterization and simultaneous electrochemical detection of ascorbic acid, dopamine and uric acid. *RSC Adv* 3:14428
40. Katoch A, Burkhart M, Hwang T, Kim SS (2012) Synthesis of polyaniline/TiO₂ hybrid nanoplates via a sol-gel chemical method. *Chem Eng J* 192:262
41. Li F, Jiang X, Zhao J, Zhang S (2015) Graphene oxide: a promising nanomaterial for energy and environmental applications. *Nano Energy* 16:488
42. Zhao D, Sheng G, Chen C, Wang X (2012) Enhanced photocatalytic degradation of methylene blue under visible irradiation on graphene@TiO₂ dyade structure. *Appl Catal B Env* 111:303
43. Selvin SSP, Kumar AG, Sarala L, Rajaram R, Sathiyam A, Princy Merlin J, Lydia IS (2018) Photocatalytic degradation of rhodamine B using zinc oxide activated charcoal polyaniline nanocomposite and its survival assessment using aquatic animal model. *ACS Sust Chem Eng* 61:258

Publisher's Note Springer Nature remains neutral with regard to jurisdictional claims in published maps and institutional affiliations.